Progress Report

for 2013 - 2016

for the Project:

Theoretical Modeling of the Magnetic Behavior of Rapidly Solidified Ferromagnetic Amorphous Submicron Wires and Nanowires

Project code: PN-II-ID-PCE-2012-4-0424

Contract no. 46/2013

– 2016 –

Table of Contents

1. Project objectives

The main objective of this project is to achieve a model for the description of the magnetic behavior of amorphous glass-coated nanowires and submicron wires prepared by rapid quenching from the melt. This main objective envisages two major directions:

(i) the analytical modeling of their domain structures and magnetic anisotropy distributions; and

(ii) the numerical simulation of the magnetic hysteresis loops of the rapidly solidified amorphous nanowires and submicron wires.

The **associate objective** is to verify experimentally the calculated and simulated results.

2. 1st stage (2013)

During the first stage of the project (September – December 2013), we have calculated the radial distributions of internal stresses induced during the preparation of the rapidly solidified amorphous nanowires and submicron wires with various dimensions (diameter of the metallic nucleus between 50 and 950 nm and glass coating thickness between 1 and 20 μm). This activity was the first step towards achieving the first specific objective, i.e. the analytical calculation of the magnetoelastic and magnetostatic terms for amorphous nanowire and submicron wire samples with various dimensions and different compositions.

In order to calculate the distributions of the internal stresses in various cases, we have assumed the preparation method – the glass-coated melt-spinning technique – as two separate phenomena, each being responsible for inducing internal stresses: (i) the rapid solidification of the actual metallic wire (i.e., of the metallic nucleus) from the temperature of the molten alloy, T_m, to the glass transition temperature, T_g, and (ii) the slow cooling of the metal-glass ensemble from the glass transition temperature, T_g, to the room temperature, T_{rt}. We have described mathematically the two phenomena (the rapid solidification T_m -> T_g and the slow cooling T_g -> T_{rt}) and we calculated separately the internal stresses induced in each step, and then we added the two separate contributions in order to obtain the distribution of the total internal stresses induced during the preparation of the nanowires/submicron wires. All the calculations have been performed in cylindrical coordinates, r, θ, and z, due to the symmetry of the samples, and we have calculated the diagonal components of the elastic stress tensor, $\overleftrightarrow{\tau}$, i.e. the radial ($\tau_{rr}$), axial ($\tau_{zz}$), and circumferential (azimuthal - $\tau_{\theta\theta}$) components, respectively.

All the equations have been solved numerically, and the entire formalism has been written into a home-made computer code, which allowed us to calculate the internal stresses for nanowires/submicron wires with any diameter from the range

between 50 and 950 nm. The glass coating thickness has been varied between 1 and 20 μm. These dimensions cover the entire range of potential values for the investigated materials.

The shapes of the calculated radial distributions of the diagonal elastic stress tensor components are similar in all the considered cases, with the axial component, τ_{zz}, being preponderant on 80 to 95% of the nanowire radius. Since the mechanical elastic stresses are tensor components, it means that τ_{zz} has the largest impact on the magnetoelastic anisotropy of the analyzed amorphous nanowires and submicron wires. The values of τ_{zz} in the nanowires is significantly larger than in the submicron wires.

From the dependence of maximum values of τ_{zz} on the diameter of the metallic nucleus, with the glass coating thickness as a parameter, we have established that the sample dimensions are essential for the magnitude of the elastic stresses induced during their preparation. Thus, for a glass coating thickness between 5 and 20 μm, its influence on the radial distribution of the internal stresses is negligible. On the other hand, when the glass coating thickness is below 5 μm, it significantly affects the distribution of the elastic stresses, which is also influenced by the diameter of the actual nanowire/submicron wire, i.e. of the metallic nucleus. These differences emphasize the efficiency of thinning the glass coating or even its complete removal in controlling the distribution of the residual stresses in rapidly solidified amorphous nanowires and submicron wires, with effects on their magnetic characteristics.

Thus, the results we have obtained during the first stage of the project were an important step towards understanding and controlling the magnetic behavior of the rapidly solidified amorphous nanowires and submicron wires, being at the same time key for the activities to be performed in the second stage of the project (2014).

The results of the elastic stress tensor components calculations in amorphous nanowires/submicron wires with various dimensions have been published in *Journal of Applied Physics*, vol. 115, no. 17, art. no. 17A329, in May 2014, in the paper entitled “Intrinsic domain wall pinning in rapidly solidified amorphous nanowires”.

3. 2nd stage (2014)

In the second stage of the project, in 2014, we have capitalized on the results obtained in the first stage and continued with the analytical calculation of the magnetoelastic and magnetostatic energy terms in the rapidly solidified amorphous submicron wires and nanowires with various dimensions and different compositions.

The activities that have been performed in this second stage were: (i) the calculation of the radial distribution of the magnetoelastic energy density for samples in which we have calculated the distribution of the elastic stress tensor components in the first stage, and (ii) the calculation of the actual magnetoelastic

energy (E_{me}) and magnetostatic energy (E_{ms}) terms, followed by a comparison of the two terms in the analyzed cases.

The first step was to choose the different alloy compositions so that the values of the magnetostriction constant in the analyzed cases are significantly different. For each composition, we have studied the evolution of the magnetoelastic and magnetostatic terms for the entire range of dimensions of the nanowires and submicron wires. The compositions we have chosen are: (i) $Fe_{77.5}Si_{7.5}B_{15}$ – a highly magnetostrictive alloy with the magnetostriction constant $\lambda = +25 \times 10^{-6}$, and (ii) $(Co_{0.94}Fe_{0.06})_{72.5}Si_{12.5}B_{15}$ – a nearly zero magnetostrictive alloy with the magnetostriction constant $\lambda \cong -1 \times 10^{-7}$.

We have calculated the magnetoelastic term starting from the elastic stress tensor components calculated in 2013. For every amorphous nanowire or submicron wire that we have considered, we averaged the preponderant component of the stress tensor, i.e. the axial one, τ_{zz}, and then, we calculated the average density of magnetoelastic energy $\varepsilon_{me} = E_{me}/V$, in which V was the sample volume:

$$\langle \varepsilon_{me} \rangle = \frac{3}{2} \cdot \lambda \cdot \langle \tau_{zz} \rangle \quad (1)$$

We observed that small values of the glass coating thickness generally yield small values of the magnetoelastic energy density. Nevertheless, this rule is not valid for very thin nanowires, e.g. a sample with 90 nm in diameter, which exhibits an unexpected maximum of the energy density at very small glass coating thicknesses. The origin of this maximum is not entirely clear, although it has been ascribed to the nonlinear dependence of the diagonal internal stress components on the glass coating thickness (elastic stresses induced during the preparation of the nanowires/submicron wires).

The calculation of the magnetostatic term from the $Fe_{77.5}Si_{7.5}B_{15}$ amorphous nanowires and submicron wires prepared by rapid solidification was made in the hypothesis that the samples are uniformly magnetized along their longitudinal axis, considered to be parallel to the *z* axis. Such a hypothesis is in agreement with the bistable magnetic behavior of these materials. Under these circumstances, the average demagnetizing field on the axial direction is:

$$\langle H_z \rangle = -\frac{M_z}{L}\left(L + R_m - \sqrt{R_m^2 + L^2}\right) \quad (2)$$

in which M_z is the axial component of the sample's magnetization, *L* the sample length, and R_m the radius of the metallic nucleus.

Taking into account that the length of any rapidly solidified amorphous nanowire or submicron wire prepared by rapid quenching from the melt is much larger than its radius ($L \gg R_m$), equation (2) becomes:

$$\langle H_z \rangle = -M_z \cdot \frac{R_m}{L} \quad (3)$$

Thus, the average magnetostatic energy density, $\langle \varepsilon_{ms} \rangle$, can be written as:

$$\langle \varepsilon_{ms} \rangle = -\frac{\mu_0}{2} \cdot \langle H_z \rangle \cdot M_z = \frac{\mu_0}{2} \cdot M_s^2 \cdot \frac{R_m}{L} \quad (4)$$

subject to the sample being saturated on the axial direction ($M_z \equiv M_s$). μ_0 is the magnetic permeability of free space ($4\pi \times 10^{-7}$ Hm^{-1}).

We have calculated the average density of magnetostatic energy for samples with different lengths and diameters.

We have established that the magnetostatic term has a significant contribution in the case of short and average length nanowires, its value being affected by both axial and transversal dimensions of the samples. As opposed to the case of the magnetoelastic term, in the case of the magnetostatic one, the thickness of the glass coating is irrelevant.

The results that we have obtained following this activity have shown that the magnetoelastic term, $\langle \varepsilon_{me} \rangle$, is always larger than the magnetostatic one, $\langle \varepsilon_{ms} \rangle$, in the case of magnetostrictive amorphous nanowire and submicron wire samples. This is valid even for samples with larger diameters of the metallic nucleus and smaller values of the glass coating thickness, such as the sample with a 950 nm nucleus diameter and a 100 nm glass coating thickness, in which the two terms have the closest possible values, namely $\langle \varepsilon_{ms} \rangle$ = 484.5 J/m^3 (for $L = L_{min}$) and $\langle \varepsilon_{me} \rangle$ = 26 kJ/m^3, respectively. But even in this case, the magnetoelastic term is two orders of magnitude larger than the magnetostatic one. Hence, the domain structure formation is determined by the minimization of the magnetoelastic energy term in the case of rapidly solidified amorphous nanowires and submicron wires with high magnetostriction.

For the same reason, the dominant magnetic anisotropy in such samples is also of magnetoelastic origin. However, taking into account the relatively large value of the magnetostatic term in shorter samples with larger diameters, it is obvious that the magnetostatic energy exerts a certain influence on their magnetic behavior, which cannot be fully neglected.

Thus, the analysis of the magnetoelastic and magnetostatic terms in amorphous nanowires and submicron wires prepared by rapid quenching from the melt, emphasizes a complex picture of the magnetic domain structure formation and of the distribution and origin of the magnetic anisotropy, a picture in which both terms play a very important role. Thus, the single-domain type magnetic domain structure with a uniaxial magnetic anisotropy along the wire axis appears because of the minimization of the magnetoelastic energy term in the volume of the samples, whilst towards the wire surface, the anisotropy distribution is the result of the magnetostatic energy minimization. The value of the switching field is determined by the preponderant term, i.e. the magnetoelastic one.

The calculated results allowed us to understand the experimental data obtained through hysteresis loop measurements. The study that we have performed also allowed us to understand the phenomena underlying the magnetic behavior of highly magnetostrictive amorphous nanowires and submicron wires prepared by rapid quenching from the melt.

If in the case of magnetostrictive samples (nanowires and submicron wires) we have found the preponderant magnetoelastic term to be at the origin of their magnetic bistability, in the case of nearly zero samples – in which the magnetostriction constant of $(Co_{0.94}Fe_{0.06})_{72.5}Si_{12.5}B_{15}$ wires is about 250 times smaller in comparison with that of $Fe_{77.5}Si_{7.5}B_{15}$ ones – a separate analysis was required in order to investigate the contribution of the magnetostatic and magnetoelastic contributions in the total free energy, in order to understand the origin and characteristics of their magnetic bistability.

We have calculated the magnetoelastic term using the same method as in the case of the magnetostrictive samples, namely starting from the radial distributions of the diagonal components of the elastic stress tensor. The next step was to average the preponderant diagonal component of the distribution, and to calculate the average magnetoelastic energy density $\langle \varepsilon_{me} \rangle$:

$$\langle \varepsilon_{me} \rangle = \frac{3}{2} \cdot \lambda'(\tau) \cdot \langle \tau_{ii} \rangle \quad (5)$$

in which $\langle \tau_{ii} \rangle$ represents the average value of the preponderant diagonal component of the stress tensor (i can be r, θ or z), whilst $\lambda'(\tau)$ is the modified magnetostriction constant, which depends on the mechanical stress. This is, in fact, the major difference with respect to the calculation of the magnetoelastic term in magnetostrictive amorphous nanowires and submicron wires: in the case of the nearly zero magnetostrictive ones, there is a stress dependence of the magnetostriction constant, which applies to both external and internal stresses (such as those induced at nanowire preparation), and which has been experimentally observed during magneto-impedance and magnetic permeability measurements. Therefore, we have considered a linear dependence of the magnetostriction constant on the average axial tensile stress, $\langle \tau_{zz} \rangle$, which, in this case, is again the dominant diagonal component of the elastic stress tensor.

Similar to the case of magnetostrictive nanowires and submicron wires, a small glass coating thickness leads to small values of the magnetoelastic term. We must emphasize however, that, as expected, the magnetoelastic energy density in nanowires and submicron wires with nearly zero magnetostriction is much smaller than in magnetostrictive ones, due to the much smaller value of the magnetostriction constant.

The calculation of the magnetostatic term, $\langle \varepsilon_{ms} \rangle$, has been achieved in a similar way to the case of the magnetostrictive amorphous nanowires and submicron wires.

We observed that the magnetostatic term is more important in the case of shorter samples with larger diameters, its value being affected by both dimensions (length and diameter). However, the most important element in this case is that the magnetostatic term is of the same order of magnitude as the magnetoelastic one, $\langle \varepsilon_{ms} \rangle \sim \langle \varepsilon_{me} \rangle$, this situation being specific only to the nearly zero magnetostrictive nanowires and submicron wires, without any possibility of appearing in the case of the magnetostrictive ones, in which the magnetoelastic term is always larger than the magnetostatic one with at least two orders of magnitude.

At the same time, we observed that the magnetostatic term is preponderant in all cases, except for metallic nucleus diameters smaller than 200 nm, when the glass coating thickness exceeds 7.5 μm. However, since any complex magnetic structure which is different from the single-domain one with uniaxial anisotropy, and which would be the result of the magnetoelastic energy minimization, would also include magnetic domain walls, and, therefore, the magnetostatic term $\langle \varepsilon_{ms} \rangle$ would increase significantly, one can state that, for nearly zero magnetostrictive rapidly solidified amorphous nanowires and submicron wires, the magnetostatic term is the one that plays the preponderant role in the formation of their magnetic domain structure.

This is also the main reason for the important differences between the switching field values in amorphous nanowire and submicron wire samples prepared from the two analyzed compositions: the magnetoelastic term and the corresponding magnetoelastic anisotropy are dominating the magnetic behavior and properties of the magnetostrictive samples, i.e. $Fe_{77.5}Si_{7.5}B_{15}$ ones, which exhibit very large values of the switching field (thousands of A/m), whilst the magnetostatic term dominates the magnetic behavior of the nearly zero $(Co_{0.94}Fe_{0.06})_{72.5}Si_{12.5}B_{15}$ samples, resulting in much smaller values of the switching field (100 – 500 A/m), and in magnetically softer overall properties.

The analysis of the two key terms from the total free energy of the amorphous nanowires and submicron wires prepared by means of rapid quenching from the melt, i.e. of the magnetoelastic and magnetostatic ones, respectively, allowed us to understand the underlying phenomena that cause their magnetic behavior, mainly their magnetic bistability, as well as to understand the basic aspects of their domain structure formation and the origin of their magnetic anisotropy, along with the differences between the switching field values in magnetostrictive and nearly zero magnetostrictive samples. All these things are extremely important for the optimization and control of their magnetic properties, as well as for the development of future applications based on these new amorphous nanowires and submicron wires, such as novel magnetic micro and nanosensors, domain wall logic applications, etc.

Consequently, all the activities planned for 2013 and 2014 have been successfully implemented.

As concerns the dissemination of the results, in the first 2 stages we have published 4 articles based on the results obtained in the project, 2 in Journal of Applied Physics and 2 in IEEE Transactions on Magnetics:

1. T.-A. Óvári and H. Chiriac, Intrinsic domain wall pinning in rapidly solidified amorphous nanowires, *J. Appl. Phys.* 115 (2014) 17A329, DOI: 10.1063/1.4866551.
2. T.-A. Óvári, N. Lupu, S. Corodeanu, and H. Chiriac, Magnetostatic and magnetoelastic interactions in glass-coated magnetostrictive nanowires, *IEEE Trans. Magn.* 50 (2014) 2006904, DOI: 10.1109/TMAG.2014.2320301.

3. T.-A. Óvári and H. Chiriac, Origin of magnetic bistability in rapidly solidified (Co0.94Fe0.06)72.5Si12.5B15 nearly zero magnetostrictive amorphous nanowires, *J. Appl. Phys.* (2015) 17D502, DOI: 10.1063/1.4906298.
4. T.-A. Óvári, S. Corodeanu, C. Rotărescu and H. Chiriac, Magnetization reversal in zero-magnetostrictive rapidly solidified amorphous nanowires, *IEEE Trans. Magn.* (2014) 2007304, DOI: 10.1109/TMAG.2014.2325131.

Besides these 4 articles, we have also finalized a book chapter for Woodhead Publishing (U.K.), which from 2013 belongs to the Elsevier group. The chapter is entitled *"Magnetic nanowires and submicron wires prepared by quenching and drawing technique"*, (chapter 7, pp. 199-223, in the book entitled *"Magnetic nano- and microwires: Design, synthesis, properties and applications"*, edited by Prof. Manuel Vázquez Villalabeitia from Instituto de Ciencia de Materiales de Madrid ICMM-CSIC, Spain. The book has been published in May 2015 (ISBN 978-0-08-100164-6).

The results obtained in 2013 and 2014 have been also disseminated through presentations at prestigious conferences in the field of magnetism and magnetic materials. The results from 2013 were presented at the 58th Annual Magnetism & Magnetic Materials Conference MMM 2013 (1 presentation), November 4 – 8, 2013, Denver, Colorado, U.S.A. The results from 2014 have been communicated at Intermag Europe – The IEEE International Magnetics Conference, Dresden, Germany, May 4 – 8, 2014 (2 presentations), at the 10th European Conference on Magnetic Sensors and Actuators EMSA 2014, July 6 – 9, 2014, Vienna, Austria (1 presentation) and at the 59th Annual Magnetism & Magnetic Materials Conference MMM 2014, November 3 – 7, 2014, Honolulu, U.S.A. (1 presentation), bringing the total number of communications on this topic to 5.

4. 3rd stage (2015)

The aim of the 2015 stage (3rd) was to numerically simulate the magnetic hysteresis loops of amorphous nanowires and submicron wires prepared by rapid solidification. The simulated cases have been correlated with the samples selected for the analytical calculations in the 2nd stage of the project (2014).

The planned activities referred to the development of a micromagnetic code for the simulation of the magnetic hysteresis and of the magnetization processes in these novel magnetic materials.

The compositions of the amorphous nanowires and submicron wires selected for the simulations of the hysteresis loops were identical to those used in the calculations of the magnetoelastic and magnetostatic terms in 2014, i.e. $(Co_{0.94}Fe_{0.06})_{72.5}Si_{12.5}B_{15}$ – with the magnetostriction constant $\lambda \cong -1 \times 10^{-7}$ and $Fe_{77.5}Si_{7.5}B_{15}$ – with the magnetostriction constant $\lambda \cong +25 \times 10^{-6}$.

For the nearly zero magnetostrictive nanowires and submicron wires having the representative composition $(Co_{0.94}Fe_{0.06})_{72.5}Si_{12.5}B_{15}$, we employed the finite differences method (FDM) to micromagnetically simulate their axial hysteresis

loops. With this aim, we developed an “in-house” micromagnetic code to numerically solve the equilibrium equations for the magnetization and to find the equilibrium distribution of the elementary magnetic moments which corresponds to the minimum energy state of the system at each value of the axially applied magnetic field, H_{ext}.

The micromagnetic equation of equilibrium, $\vec{M} \times \vec{H}_{eff} = 0$, in which $\vec{M}$ is the magnetization vector, and $\vec{H}_{eff} = -\partial E/\partial M$ is the effective magnetic field, E being the total free energy of the system, has been solved using a system of nonlinear algebraic equations which results following the discretization of the investigated nanowires into very small elementary cells with dimensions smaller than the exchange length of each material considered, $L_{ex} = \sqrt{2A/\mu_0 M_S^2}$, in which A is the exchange parameter, μ_0 the magnetic permeability of vacuum, and M_S the saturation magnetization.

Each discretization cell has its own elementary magnetic moment, so that the nanowire can be considered as a system of elementary magnetic moments or dipoles, $\vec{\mu}$. For the $(Co_{0.94}Fe_{0.06})_{72.5}Si_{12.5}B_{15}$ nanowires, we employed discretization cells with the dimension of 4 nm, which is well below the exchange length for this alloy, i.e. $L_{ex} \cong 7$ nm.

The technique that we have employed in order to simulate the loops was to align simultaneously, but gradually, the magnetic moments of all the dipoles within the system, $\vec{\mu}(i,j,k)$, that correspond to all the discretization cells within a sample, with the local direction of the effective field, $\vec{H}_{eff}(i,j,k)$, technique which is also known as the Jacobi method. The effective field is given by:

$$\vec{H}_{eff} = \vec{H}_{ex} + \vec{H}_d + \vec{H}_{ext} \qquad (6)$$

where the first term represents the exchange interaction, the second one is the demagnetizing one (magnetostatic interaction), and the last one represents the interaction with the applied field, also called the Zeeman term.

The term given by the magnetoelastic anisotropy has been neglected in a first approximation, given the extremely small value of the magnetostriction constant (in this case we can consider $\lambda \cong 0$). The magnetocrystalline anisotropy is null, since all the investigated samples are amorphous.

The exchange term has been calculated considering only the interaction with the first order neighbors, i.e., for the elementary moment $\vec{\mu}(i,j,k)$, the interaction with the magnetic moments corresponding to cells $i-1$ and $i+1$ on x, with those corresponding to cells $j-1$ and $j+1$ on y, and with those corresponding to cells $k-1$ and $k+1$ on the z axis.

The demagnetizing term has been calculated in the dipolar approximation, considering the interaction among the magnetic moment that corresponds to the current cell, $\vec{\mu}(i,j,k)$, and all the other magnetic moments from the system, i.e. $\sum_{i',j',k'} \vec{\mu}\,(i',j',k')$, with $i \neq i'$, $j \neq j'$ and $k \neq k'$.

The system of elementary magnetic moments was considered to be in equilibrium when:

$$\left|\mu \times H_{ef}\right| < \varepsilon \qquad (7)$$

was sufficiently small in the entire system. We have chosen the optimum value $\varepsilon = 10^{-5}$, for which we considered the convergence criterion given by (7) to be fulfilled.

We have analyzed the dependence of coercivity on nanowire dimensions in order to understand the basic aspects of their magnetization processes in the case of nearly zero magnetostrictive samples prepared by rapid quenching from the melt.

We have simulated the hysteresis loops of nearly zero magnetostrictive nanowires using the method described above. The method has been applied to samples having various lengths. The sample length has been modified in order to account for the changes in the magnetostatic term in the simulations, when the sample diameter is constant. We have chosen to keep the wire radius, R, constant, and at a relatively small value, in order to achieve reasonable processing times for the micromagnetic codes, and without affecting the accuracy of the simulations.

Figure 1 shows several simulated hysteresis loops for nearly zero magnetostrictive $(Co_{0.94}Fe_{0.06})_{72.5}Si_{12.5}B_{15}$ amorphous glass-coated nanowires. For simplicity, we have assumed that the samples are uniformly magnetized in the initial state. To reverse the magnetization of a uniformly magnetized nanowire, it is necessary to nucleate first a domain with reversed magnetization, followed by the propagation of the 180° domain wall between this domain and the rest of the sample's magnetization, as illustrated schematically in figure 2. The nucleation field, H_N, is quite large, and, therefore, the coercivity is also important.

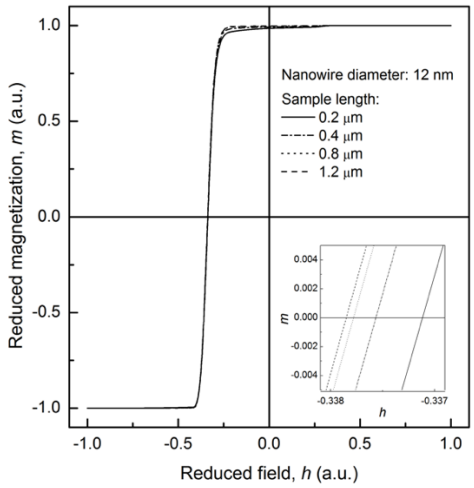

Figure 1. Numerically simulated magnetic hysteresis loops for $(Co_{0.94}Fe_{0.06})_{72.5}Si_{12.5}B_{15}$ rapidly solidified amorphous nanowires with nearly zero magnetostriction. The diameter of the simulated samples was 12 nm, whilst the length was varied between 0.2 and 1.2 μm.

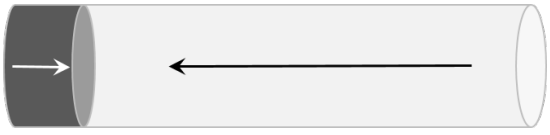

Figure 2. Nucleation of a domain with reversed magnetization in a nanowire.

We have analyzed the results using dimensionless quantities: $m = M/M_S$, the reduced magnetization, and $h = H_{ext}/H_{ext}^{max}$, the reduced applied external field.

In the inset of figure 1 we have represented the near-coercivity region. One observes that coercivity increases with the sample length, L. The detailed analysis of this dependence has revealed the role of the magnetostatic energy and of the associated anisotropy (shape anisotropy) in the magnetization process of nearly zero magnetostrictive amorphous nanowires. Thus, an increment in the sample length, L, is equivalent to a decrease of the magnetostatic energy in the case of long and thin ferromagnetic cylinders (with small diameters), i.e. in the case of those for which we can write $L \gg R$, since $\left|\vec{H}_d\right| = H_d \sim R/L$. Hence, the results shown in figure 1 indicate that coercivity increases monotonically with the decrease of the magnetostatic term, provided that the magnetoelastic term is null. Thus, it is possible to have an increase in coercivity even as a result of a decrease in the magnetostatic energy term.

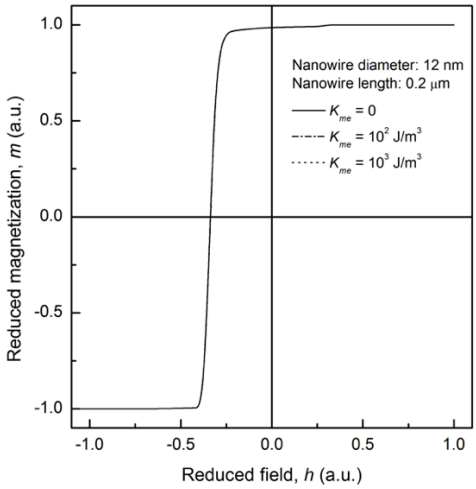

Figure 3. Simulated hysteresis loops for $(Co_{0.94}Fe_{0.06})_{72.5}Si_{12.5}B_{15}$ amorphous nanowires with low variable magnetoelastic anisotropy. The diameter of the simulated samples was 12 nm and their length was 0.2 μm.

To demonstrate the validity of the chosen methodology, as well as of the theoretical hypotheses, we have considered in the calculations the effect of a small magnetoelastic anisotropy, suitable for the nearly non-magnetostrictive alloy, in order to study its effect on the hysteresis loops of the nearly zero magnetostrictive amorphous nanowires prepared by rapid quenching from the melt. The corresponding simulated loops are shown in figure 3. The simulated sample is a nanowire with 12 nm in diameter and 0.2 μm in length. The value of the magnetoelastic anisotropy constant, K_{me}, has been varied between 0 and 10^3 J/m^3. Since $K_{me} = (3/2) \cdot \lambda \cdot \langle\tau\rangle$, in which $\langle\tau\rangle$ is the average value of the preponderant diagonal component of the elastic stress tensor (internal stresses induced at preparation), these are plausible values for the magnetoelastic anisotropy constant. We have also considered the possible change in the sign of the magnetostriction constant due to the effect of the very large internal stresses (several GPa), but taking care to keep its absolute value sufficiently low, as in the real cases, i.e. $\lambda \rightarrow +1 \times 10^{-7}$.

The results illustrated in figure 3 show that such a small magnetoelastic anisotropy does not affect the coercivity, nor the squareness of the loops, i.e. the ratio between remanence and saturation, M_R/M_S. Thus, one can state that the results shown in figure 1 are sufficiently accurate, even in the simplified assumptions that we have considered.

Summarizing, in the case of the nearly zero magnetostrictive nanowires prepared by rapid solidification techniques, the changes in the magnetostatic term represent in fact changes in the shape anisotropy, which appear as a result of the changes in the sample dimensions (diameter, length), and, most important, which can appear in the absence of any other type of magnetic anisotropy, including the magnetoelastic one.This result demonstrates the importance of shape anisotropy in the rapidly solidified amorphous nanowires, and it also shows that a strong specific anisotropy, such as the magnetoelastic one, is not a prerequisite for the appearance of the magnetic bistability.

Moreover, the squareness ratio, M_R/M_S, offers additional evidence for the important role played by shape anisotropy in the magnetic behavior of nearly zero magnetostrictive amorphous nanowires. This ratio increases slightly with the sample length, L, clearly showing that it is a consequence of $L \gg R$, i.e. of the shape anisotropy.

To calculate the hysteresis loops of $Fe_{77.5}Si_{7.5}B_{15}$ nanowires, with a large and positive magnetostriction constant ($\lambda \cong +25 \times 10^{-6}$), we have employed the same methodology, except that we included from the beginning the anisotropy term, $\vec{H}_K$, in the expression of the effective field:

$$\vec{H}_{eff} = \vec{H}_{ex} + \vec{H}_K + \vec{H}_d + \vec{H}_{ext} \quad (8)$$

This term refers strictly to the magnetoelastic anisotropy, much larger in this case due to the larger magnetostriction.

The simulation results for a 0.2 μm long $Fe_{77.5}Si_{7.5}B_{15}$ amorphous nanowire with the diameter of 12 nm are shown in figure 4 below. The value of the magnetoelastic anisotropy constant has been varied between 0 and 10^5 J/m^3, which cover the entire range of potential values for K_{me}. In the bottom inset one can observe that anisotropy constants up to 10^4 J/m^3 do not influence the coercivity. However, a value of K_{me} of 10^5 J/m^3 leads to a significant increase in coercivity, showing the importance of the magnetoelastic term in the high-field magnetization processes. In the upper inset, one observes the effect of the magnetoelastic term on the value of the squareness ratio, M_R/M_S, which increases monotonically with K_{me}. For the high-field magnetization processes, the ratio M_R/M_S measures the ease of nucleation, namely how easily a domain with reversed magnetization is formed. Hence, using micromagnetic simulations, we have identified a direct connection between coercivity, through the nucleation field, and the magnetoelastic term.

In order to reveal the influence of the magnetostatic term, through the shape anisotropy, on coercivity, we have modified in a first step the sample length from 0.2 μm to 1 μm. The results are illustrated in figure 5.

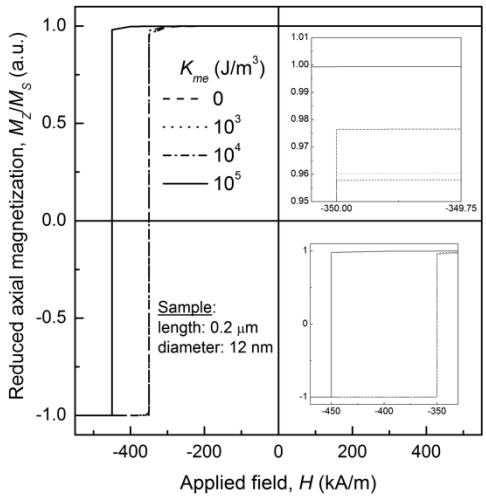

Figure 4. Simulated hysteresis loops in the case of a rapidly solidified amorphous $Fe_{77.5}Si_{7.5}B_{15}$ nanowire with the metallic nucleus diameter of 12 nm and the sample length of 0.2 μm, with the magnetoelastic anisotropy constant as a parameter.

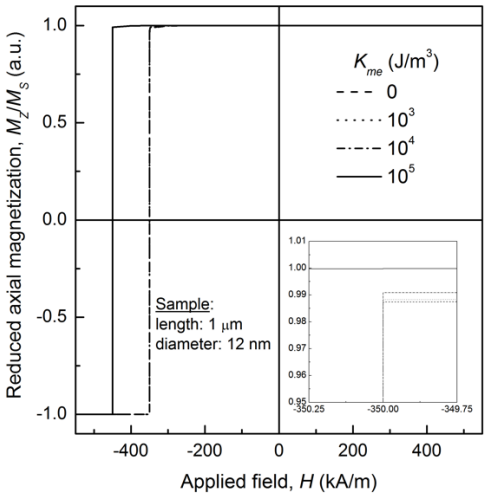

Figure 5. Simulated loops for a rapidly solidified amorphous $Fe_{77.5}Si_{7.5}B_{15}$ nanowire having 12 nm in diameter and 1 μm in length, with the magnetoelastic anisotropy constant as a parameter.

The next step was to increase the nanowire diameter from 12 nm to 50 nm, keeping the sample length constant at 1 μm. The results of these simulations are shown in figure 6.

We observe that the simple increase in sample length, even 5 times, does not affect the value of the coercivity. This result validates the use of 0.2 μm long samples for the initial calculations. On the other hand, the increase in the squareness, M_R/M_S, shows a more important contribution of the magnetostatic term (shape anisotropy) to the nucleation field. As concerns the magnetoelastic term, one can observe that even for longer samples the variation of M_R/M_S with K_{me} is maintained, but it is less pronounced than in the case of the shorter sample (L = 0.2 μm).

On the other hand, according to the results illustrated in figure 6, an increment of the sample diameter up to 50 nm leads to a significant decrease in coercivity in

comparison with the case of the sample with 12 nm in diameter. This shows that it is much easier to nucleate a reverse domain in thicker nanowires, and it is in agreement with the smaller values of M_R/M_S. Nevertheless, magnetoelastic anisotropy constants up to 10^4 J/m^3 still do not affect the value of the coercivity.

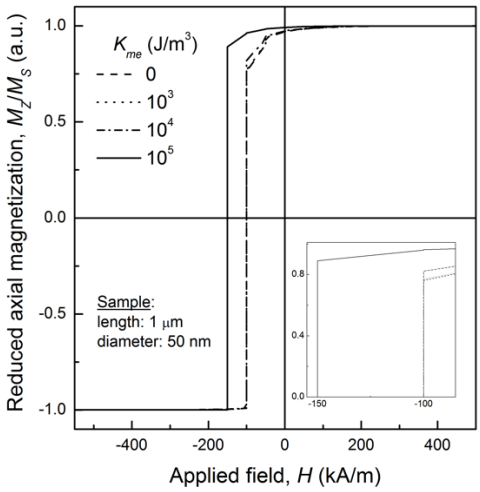

Figure 6. Simulated loops for a rapidly solidified amorphous $Fe_{77.5}Si_{7.5}B_{15}$ nanowire having 50 nm in diameter and 1 μm in length, with the magnetoelastic anisotropy constant as a parameter.

Summarizing, in the case of the magnetostrictive amorphous nanowires, the micromagnetic simulation of their magnetization processes, along with the experimental hysteresis loops show that their magnetic behavior is affected by both the magnetoelastic term and by the magnetostatic one. The magnetoelastic term modifies the value of the coercivity, irrespective of the mechanism of magnetization reversal. The magnetostatic term, on the other hand, through the associated shape anisotropy, affects the value of the nucleation field, H_N.

Hence, the magnetic behavior of nearly zero magnetostrictive nanowires is governed by the magnetostatic term, whilst the magnetic behavior of highly magnetostrictive nanowires is determined by both the magnetostatic and magnetoelastic terms. This knowledge is important for fully understanding their characteristics in order to control them and tailor them adequately for various applications. Shape anisotropy can be modified by changing the sample dimensions, whilst the magnetoelastic anisotropy can also be altered through: (i) composition, which affects the value of the magnetostriction constant; (ii) annealing (thermal, thermo-magnetic, thermo-stress-magnetic, etc.); (iii) post-production treatments, e.g. glass thinning, glass removal, etc.

These results are very important for the potential applications of these novel nanowires in new micro and nanosensing devices and in domain wall logic devices, where they could replace the more expensive planar nanowires which are prepared through various lithographic methods.

The main results obtained in the 3rd stage of the project have been included in the following two articles:

1. C. Rotărescu, A. Atițoaie, L. Stoleriu, T.-A Óvári, N. Lupu, H. Chiriac, “Shape anisotropy in zero-magnetostrictive rapidly solidified amorphous nanowires”, *Physica B-Condensed Matter*, vol. 486, Apr. 2016, pp. 73-76; and
2. T.-A. Óvári, C. Rotărescu, A. Atițoaie, S. Corodeanu, N. Lupu, and H. Chiriac, “Magnetic anisotropy in rapidly quenched amorphous glass-coated nanowires”, *J. Magn. Magn. Mater.*, vol. 410, Jul. 2016, pp. 100-104.

With these two papers, the total number of publications has reached **6 articles** (2 in *Journal of Applied Physics*, 2 in *IEEE Transactions on Magnetics*, 1 in *Physica B* and 1 in *Journal of Magnetism and Magnetic Materials*) and **one book chapter** published by Woodhead Publishing.

The results have been widely disseminated at the following international conferences:

- IEEE International Magnetics Conference – INTERMAG 2015, Beijing, China, May 11 – 15, 2015 – 2 presentations:
    - (FQ-13) Effect of magnetostriction on the low- and high-field magnetization reversal of rapidly solidified amorphous nanowires – T.-A. Óvári, C. Rotărescu, A. Atițoaie, H. Chiriac;
    - (HR-01) Anisotropy distribution in rapidly quenched amorphous glass-coated nanowires – T.-A. Óvári, S. Corodeanu, M. Lostun, G. Ababei, H. Chiriac.
- 20th International Conference on Magnetism – ICM 2015, Barcelona, Spain, July 5 – 10, 2015 – 1 presentation:
    - (Mo.K-P30) Mechanism of magnetic switching in rapidly solidified amorphous nanowires – T.-A. Óvári, C. Rotărescu, A. Atițoaie, H. Chiriac.
- IOP (Institute of Physics) Magnetism 2015, Leeds, UK, March 30 – 31, 2015 – 1 presentation:
    - (P.66) Amorphous glass-coated nanowires and submicron wires prepared by rapid quenching from the melt – M. Țibu, T.-A. Óvári, H. Chiriac.
- 10th International Symposium on Hysteresis Modeling and Micromagnetics – HMM 2015, Iași, România, May 18 – 20, 2015 – 1 presentation:
    - (P55) Shape anisotropy in zero-magnetostrictive rapidly solidified amorphous nanowires – C. Rotărescu, A. Atițoaie, L. Stoleriu, T.-A. Óvári, N. Lupu, H. Chiriac.
- 7th International Workshop on Amorphous and Nanostructured Magnetic Materials – ANMM’2015, Iași, Romania, September 21 – 24, 2015 – 2 presentations:
    - (P.30) Micromagnetic simulations of cylindrical magnetic nanowires with zero magnetostriction – C. Rotărescu, T.-A. Óvári, N. Lupu, H. Chiriac;
    - (P.35) Investigation of domain walls nucleation and motion in submicron amorphous wires – M. Țibu, M. Lostun, D.A. Allwood, N. Lupu, T.-A. Óvári, H. Chiriac.

The project activities have also contributed to the formation of 5 young postdoctoral researchers from the team, 4 of them – Dr. Cristian Rotărescu, Dr. Sorin Corodeanu, Dr. Gabriel Ababei and Dr. Mihai Țibu – being coauthors of the papers published or presented.

We also had very good international collaborations on the topics of this project, these being supported by an FP7 REGPOT type project, in which we collaborate with the group of Prof. Dan Allwood from the University of Sheffield, UK, one of the groups with an interest in the development of domain wall logic devices.

5. 4th stage (2016)

In this last stage of the project, the focus was on two activities:

1. The optimization of the micromagnetic code for the simulation of magnetic hysteresis in submicron wires and nanowires prepared by means of rapid solidification from the melt; and
2. The experimental verification of the numerically calculated and simulated results.

In order to achieve the first activity, we have considered the correlation between the discretization of the system (i.e. the nanowire or submicron wire) and the actual method implemented for the calculation of the equilibrium configuration of the magnetization in each case. The discretization and its effect on the simulation results, along with the method for the calculation of the equilibrium configuration of the magnetic moments are highly technical, but essential details, that may impact on the accuracy of the overall results.

The method for the calculation of the equilibrium configurations of the magnetic moments refers to the actual technique of solving the equilibrium equation at any value of the applied magnetic field, including H_{ext} = 0. To optimize the calculation method, we tested comparatively the following approaches:

1. The LaBonte method – in which the individual magnetic moments, from each discretization cell, are sequentially aligned with the local effective field, $\vec{H}_{ef}$, one by one, the magnetization of each cell, $\vec{\mu}$, being rotated towards the local effective field until the equilibrium condition (7) is fulfilled;
2. The Jacobi method – in which the elementary magnetic moments are simultaneously rotated towards the local effective field within the whole system (nanowire or submicron wire);
3. The Jacobi method with FFT (fast Fourier transform) – a variant of the Jacobi method in which the magnetic moments are also simultaneously rotated towards the local effective field, but the magnetostatic term, whose calculation takes most resources and is the most time consuming, is calculated using a mathematical method that implies FFT, which, in certain circumstances, can significantly reduce the processing time, but at the expense of the system memory (RAM); and

4. The Monte Carlo method – a statistical method that implies the rotation of randomly selected magnetic moments towards the local effective field.

Thus, in order to optimize the simulation by the calculation method, we selected first a test system, i.e. a nanowire with the diameter of 12 nm and 0.2 μm in length (also employed in the simulations that led to the results shown in Fig. 1, Fig. 3 and Fig. 4) and we applied all the four methods mentioned above. The results are illustrated in Fig. 7 below.

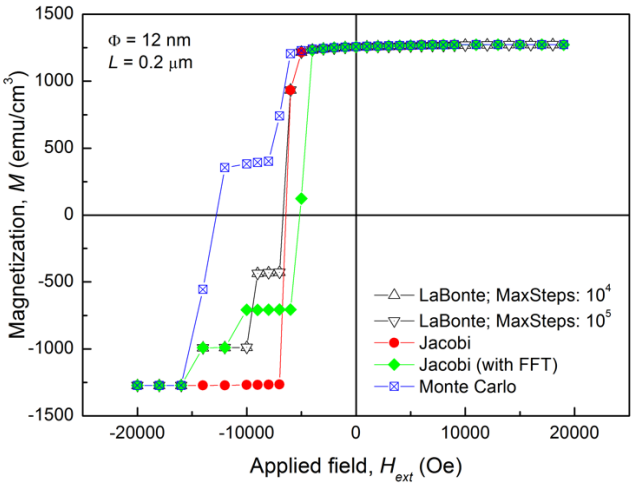

Fig. 7. Numerically simulated hysteresis loops in the case of an amorphous $Fe_{77.5}Si_{7.5}B_{15}$ rapidly solidified amorphous nanowire with 12 nm in diameter and 0.2 μm in length, using different methods for the calculation of the equilibrium configurations of the magnetization: LaBonte, Jacobi, Jacobi with fast Fourier transform (FFT) and Monte Carlo.

For the LaBonte method, we have employed in our "in-house" developed micromagnetic code, two different parameters in order to stop the oscillations of the system following too many iterations performed in order to reach equilibrium: MaxSteps = 10^4 and MaxSteps = 10^5 steps, respectively. We observed that the reduction of this parameter with one order of magnitude does not affect the precision of the calculations, however it allows one to optimize the code from the point of view of the processing time.

From Fig. 7 we notice that the standard Jacobi method (without FFT) is the most accurate and efficient for the simulation of the investigated magnetic nanowire and submicron wire systems. The other three methods, although some of them allow faster processing (Jacobi with FFT and Monte Carlo), have led to less accurate results.

In order to see if this result is general, we have applied the four simulation techniques to a longer system, i.e. a nanowire with the same diameter (12 nm), but double in length (0.4 μm). The results are shown in Fig. 8. We have noticed that the standard Jacobi method gives the best results in this case as well.

Thus, the micromagnetic code optimization from the point of view of the implemented calculation method has led us to the choice of the most accurate one, namely of the standard Jacobi method.

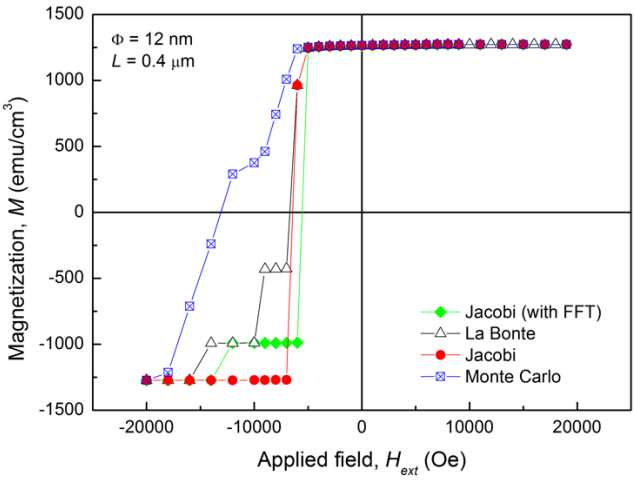

Fig. 8. Numerically simulated hysteresis loops in the case of an amorphous $Fe_{77.5}Si_{7.5}B_{15}$ rapidly solidified amorphous nanowire with 12 nm in diameter and 0.4 μm in length, using different methods for the calculation of the equilibrium configurations of the magnetization: LaBonte, Jacobi, Jacobi with fast Fourier transform (FFT) and Monte Carlo.

As concerns the second element taken into account for the optimization of the micromagnetic code, i.e. the effect of the system discretization on the results of the numerical simulations, we have investigated the role of the discretization cell size on the hysteresis loops of a simple system characterized by the same value of the exchange length, L_{ex}, as the analyzed nanowires. Hence, for $L_{ex} = 7$ nm, we have started from the same discretization cell size D = 4 nm, and we have subsequently reduced this value in steps down to D = 1 nm, which means that we had to compensate by increasing the number of the discretization elements in order to keep the same size of the studied system. The results are shown in Fig. 9.

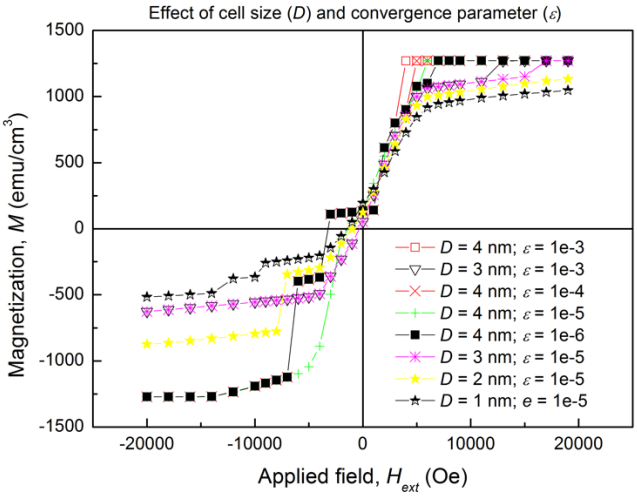

Fig. 9. Effect of cell discretization size, D, and of the convergence parameter, ε, on the micromagnetic simulations of a system with the exchange length of 7 nm.

Thus, besides the cell size, an important role is also played by the convergence parameter. Nevertheless, once these parameters are decreased, both the processing time and the required computing memory increase.

From the results illustrated in Fig. 9 we observe that the system's magnetization is fully reversed ($+M_S \rightarrow -M_S$) only when D = 4 nm, and this happens irrespective of the magnitude of the convergence parameter ε. This is a consequence of the large number of discretization cells when the cell size is small (from D = 1 nm to D = 3 nm), which results in an unstable system, in which equilibrium is hard to reach, most likely due to the large number of necessary iterations. This is also the reason for which a convergence parameter of 10^{-6} results in staired loops even in the case of D = 4 nm. The optimum value is therefore $\varepsilon = 10^{-5}$, since larger values, e.g. 10^{-4} and 10^{-3}, may alter the nucleation process. The optimum cell size is D = 4 nm.

Summarizing, the systematic study we conducted in order to optimize the micromagnetic code has given us the optimum simulation technique (the standard Jacobi method), alongside the optimum discretization cell size (D = 4 nm), but also the optimum convergence parameter and the oscillation avoidance parameter (MaxSteps).

To achieve the second activity from this stage (2016), we conducted experiments on samples with the compositions of interest, i.e. $Fe_{77.5}Si_{7.5}B_{15}$, with large and positive magnetostriction ($\lambda = 25 \times 10^{-6}$), and $(Co_{0.94}Fe_{0.06})_{72.5}Si_{12.5}B_{15}$, with small negative magnetostriction ($\lambda = -1 \times 10^{-7}$). The samples have been prepared by means of rapid solidification from the melt in our institute. They exhibit metallic nucleus diameters between 130 and 950 nm and glass coating thickness from 5 to 15 μm. We have measured their inductive hysteresis loops, along with the domain wall velocities involved in the axial magnetization process of the studied nanowires and submicron wires.

Fig. 10 (a) shows the measured inductive hysteresis loops of $Fe_{77.5}Si_{7.5}B_{15}$ amorphous submicron wire samples, whilst Fig. 10 (b) shows the field dependence of the domain wall velocity (the velocity of the domain wall that propagates along the wire axis at magnetization reversal).

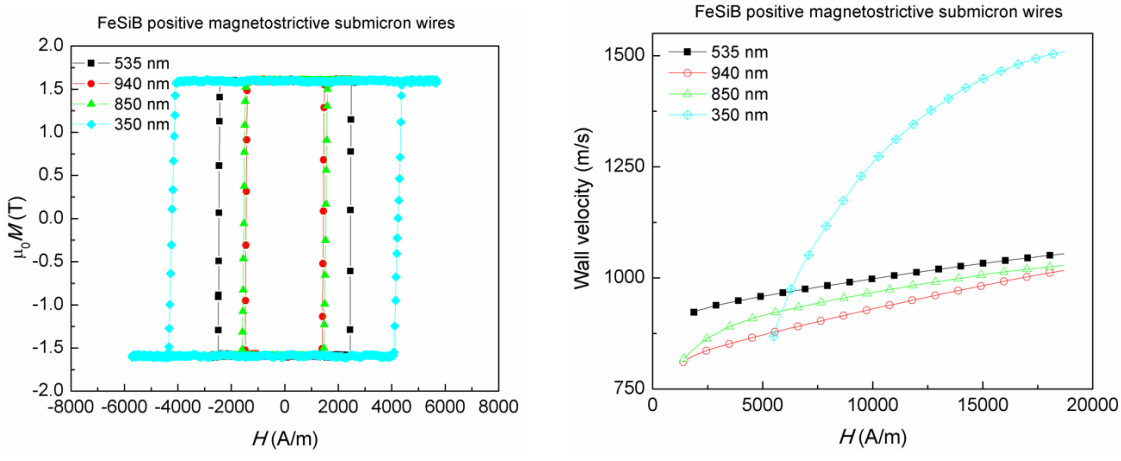

(a) (b)

Fig. 10 (a) Inductive hysteresis loops for amorphous $Fe_{77.5}Si_{7.5}B_{15}$ submicron wires. The metallic nucleus diameter varies, whilst the glass coating thickness is constant (15 μm); (b) Domain wall velocity vs. applied magnetic field for the same samples.

One observes the correlation between the domain wall velocities and the values of the switching field (the value of the applied field at which the axial magnetization reversal occurs), which confirm the equivalence of the two phenomena. Thus, larger velocities correspond to larger switching fields, which indicates a correlation between the magnitude of the axial anisotropy and the value of the wall velocity. There is also a significantly different slope in the velocity vs. field dependence of the 350 nm sample. This indicates a different axial anisotropy in this case. Taking into account the results we obtained through the micromagnetic simulations, we can state that, in the case of samples with larger diameters, the magnetic anisotropy is of magnetoelastic origin (due to the coupling between magnetostriction and internal stresses induced during preparation), whilst in the case of the thinner 350 nm sample, the magnetic anisotropy is mainly of magnetostatic origin, i.e. shape anisotropy. Thus, the effect of internal stresses is diminished once the wire diameter decreases below a certain value. Below this value, the applied field is also more effective in propagating the domain walls, which is proven by the increased domain wall velocity, v, and mobility ($\partial v/\partial H$). Therefore, an increment in the contribution of the shape anisotropy results in the increase of the domain wall mobility and velocity in the case of positive magnetostrictive samples.

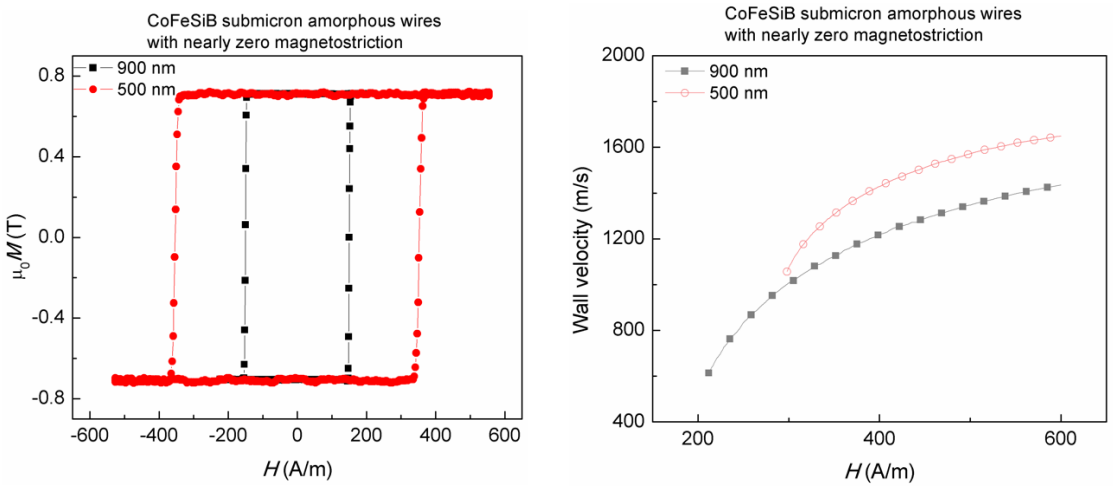

(a) (b)

Fig. 11 (a) Inductive hysteresis loops for $(Co_{0.94}Fe_{0.06})_{72,5}Si_{12,5}B_{15}$ amorphous glass-coated submicron wires with different metallic nucleus diameters (the glass coating thickness is the same: 13 μm); (b) Domain wall velocity vs. applied field for the same samples.

Fig. 11 shows the same experimental data for the $(Co_{0.94}Fe_{0.06})_{72.5}Si_{12,5}B_{15}$ submicron wires with nearly zero magnetostriction: Fig. 11 (a) the axial inductive hysteresis loops, and Fig. 11 (b) the domain wall velocity vs. applied magnetic field. The correlation between wall velocity and axial anisotropy through the value of the switching field is also observed in this case. However, only the shape anisotropy contributes this time to the larger wall velocity values, as opposed to the case of the highly magnetostrictive samples, in which there is also a significant magnetoelastic contribution, at least until the threshold value for the wire diameter. Therefore, the experimental results confirm unequivocally the calculated ones:

magnetic bistability of nearly zero magnetostrictive samples originates in the axial anisotropy of magnetostatic nature, i.e. shape anisotropy. This is also supported by the larger domain wall mobilities in the thinner wires, as explained in the case of the magnetostrictive samples with small diameters.

Taking into account these results, and, more specifically, the effect of sample dimensions on the type of preponderant magnetic anisotropy, we have continued to experimentally investigate these matters and, therefore, we decreased the diameters of the prepared samples.

Fig. 12 shows the experimental hysteresis loops for two much thinner amorphous nanowire samples prepared by rapid solidification: a highly magnetostrictive sample ($Fe_{77.5}Si_{7.5}B_{15}$) and a nearly zero magnetostrictive one $(Co_{0.94}Fe_{0.06})_{72.5}Si_{12.5}B_{15}$. Both samples are magnetically bistable, irrespective of their magnetostriction, which is in line with what we expected following the simulations and the experimental data on the thicker samples.

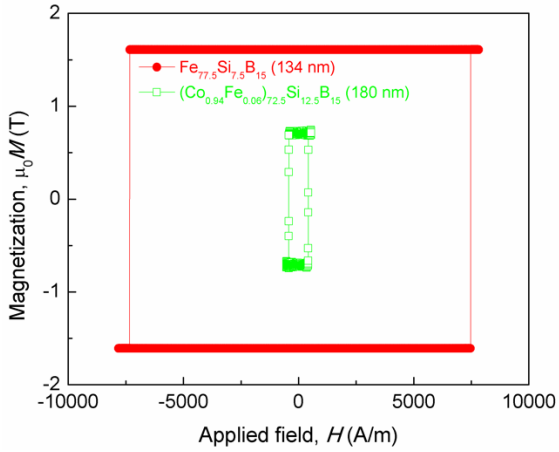

Fig. 12. Inductive hysteresis loops of two rapidly solidified amorphous nanowires: a positive magnetostrictive one with the nucleus diameter of 134 nm and the glass coating thickness of 6 μm, and a nearly zero magnetostrictive one with the nucleus diameter of 180 nm and the glass coating thickness of 5.6 μm.

There is a significant difference between the values of the switching field fpr the two samples, i.e. 420 A/m in case of the nearly zero magnetostrictive nanowire and 7400 A/m for the highly magnetostrictive one.

Fig. 13 illustrates the surface hysteresis loops for the same nanowires, measured using magneto-optical Kerr effect (MOKE) magnetometry. These results emphasize that both nanowires are magnetically bistable in their entire volume. This shows that rapidly solidified nanowires exhibit a single-domain type magnetic structure, substantially different from the core-shell type encountered in the case of typical amorphous microwires.

Thus, at the “nano” scale, the sample dimensions do not allow the formation of a complex magnetic domain structure, this fact being valid irrespective of the wire composition. We can therefore conclude that shape anisotropy, of magnetostatic origin, is preponderant within the rapidly solidified nanowires, despite the quite large

mechanical internal stresses induced during their preparation. Nevertheless, these stresses play a key role in determining the value of the switching field.

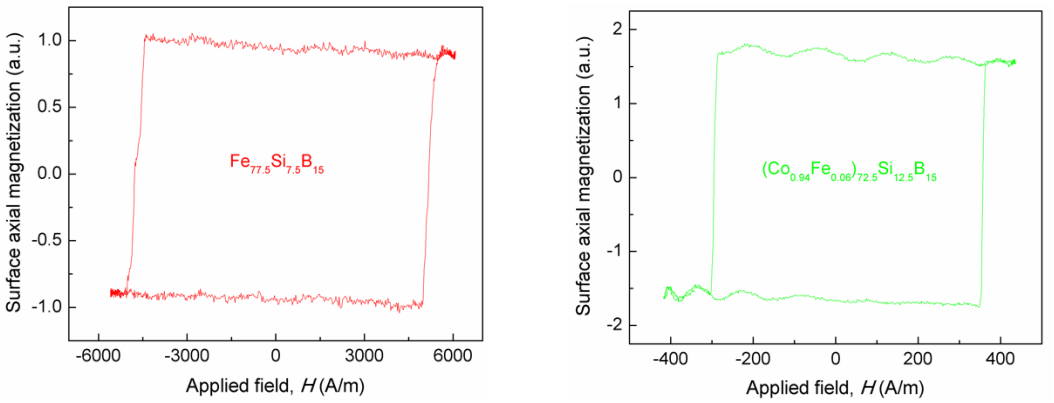

Fig. 13. Surface hysteresis loops (MOKE) for two rapidly solidified magnetic amorphous nanowires: a positive magnetostrictive one (left) and a nearly zero magnetostrictive one (right).

The direct relation between the value of the switching field and the ratio between the thickness of the glass coating and the metallic nucleus diameter is well known. $(Co_{0.94}Fe_{0.06})_{72.5}Si_{12.5}B_{15}$ nanowires display a magnetostriction constant which is one order smaller, which leads to much smaller values of the switching field, accordingly. Consequently, the value of the switching field can be tailored by changing the composition, as well as by partial or complete glass removal.

The difference between the value of the overall switching field, given by the inductive hysteresis loop, and the value of the surface switching field, given by the MOKE hysteresis loop, originates in the surface defects of the actual metallic wire (i.e., the metallic nucleus) as well as in the demagnetizing effect. Both are responsible for generating a specific magnetization distribution in the near-surface region of the metallic nanowire, which are small local deviations of the magnetization from the axial direction. They are emphasized by means of MOKE investigations, when the applied field is transverse to the nanowire axis.

In order to investigate the distribution of the anisotropy axes within the rapidly solidified nanowires, we have performed ferromagnetic resonance (FMR) measurements. The FMR investigations have been performed on highly magnetostrictive samples, the area of interest being the near-surface region, in which their stress distribution should lead to a transverse anisotropy whenever the magnetoelastic term becomes important.

Fig. 14 shows the microwave absorption resonance spectrum for an amorphous $Fe_{77.5}Si_{7.5}B_{15}$ nanowire (left). For comparison, the spectrum of a submicron amorphous wire with the same composition, but larger diameter (800 nm) is also illustrated (right).

The resonance spectrum of the submicron wire exhibits a complex maximum, which indicates a complicated anisotropy distribution within the near-surface region. This supports the above mentioned local deviations of the anisotropy axis from the axial direction. On the other hand, the resonance spectrum of the nanowire shows a simple absorption maximum, which corresponds to a single magnetic anisotropy

direction, which supports the existence of a single-domain type magnetic structure in these materials, in agreement with the results of our micromagnetic simulations. Hence, all the experimental investigations that we have performed on the rapidly solidified amorphous nanowires and submicron wires (inductive hysteresis loops, MOKE surface hysteresis loops, FMR and domain wall velocity measurements) show that these ultrathin samples exhibit a single domain magnetic structure. The experimental results confirm the calculated ones and show that shape anisotropy is essential in determining this peculiar feature.

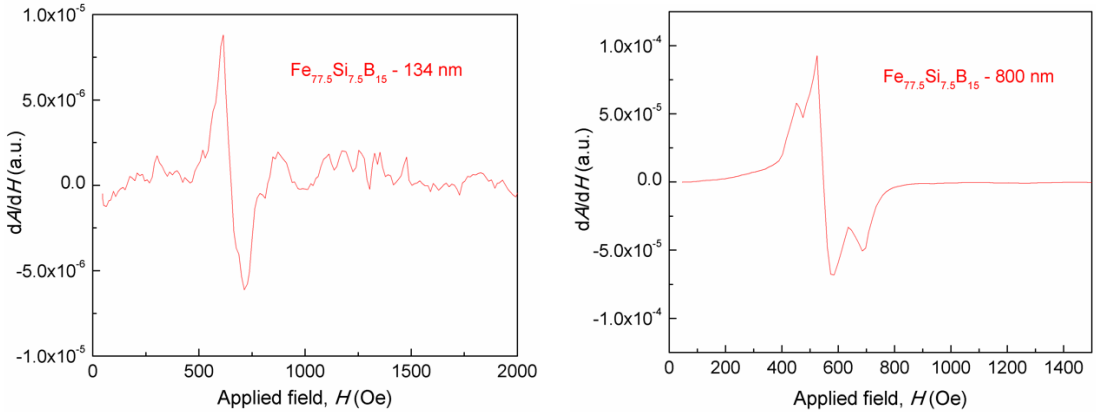

Fig. 14. Ferromagnetic resonance spectra for an amorphous $Fe_{77.5}Si_{7.5}B_{15}$ nanowire with the metallic nucleus diameter of 134 nm (left), and for a submicron amorphous wire with the same composition having 800 nm in diameter (right). Both spectra have been measured at 10.5 GHz.

Moreover, the experimental results allow one to complete the description that results from the numerical simulations with valuable data on the near-surface area of the samples, data obtained through specific techniques – MOKE and FMR – and which would be difficult to obtain otherwise.

In summary, in this last stage of the project we have achieved both planned activities – the optimization of the micromagnetic code and the experimental verification of the calculated and numerically simulated results – which emphasizes the successful completion of the project, all the initially proposed objectives being reached.

The 2016 results are included in two articles – one published in *AIP Advances* and another one submitted to *Crystals*:

1. M. Țibu, M. Lostun, D.A. Allwood, C. Rotărescu, A. Atițoaie, N. Lupu, T.-A. Óvári, H. Chiriac, "Controlled motion of domain walls in submicron amorphous wires", *AIP Advances*, vol. 6, 055922 (2016); and
2. H. Chiriac, N. Lupu, G. Stoian, S. Corodeanu, T.-A. Óvári, "Ultrathin nanocrystalline magnetic wires", *Crystals*, submitted (Dec. 2016).

The first article includes results on the axial magnetization reversal in amorphous submicron wires, specifically on the associated domain wall movements, being the result of the outstanding collaboration with the group of Professor Dan Allwood from the University of Sheffield, UK, a group with remarkable results in the field of domain wall logic devices, whilst the second one includes our most recent results on the amorphous nanowires and submicron wires

that can develop a nanocrystalline structure following an appropriate annealing procedure. Most importantly, this unique structure is reached with the preservation of magnetic bistability, which is a characteristic of the amorphous state.

The two articles have raised the total number of publications related to this project in the period 2013 – 2016 to **8 articles** (2 in *Journal of Applied Physics*, 2 in *IEEE Transactions on Magnetics*, 1 in *Physica B-Condensed Matter*, 1 in *Journal of Magnetism and Magnetic Materials*, 1 in *AIP Advances* and 1 in *Crystals*) and **a book chapter** published by Woodhead Publishing, a member of the Elsevier group.

The results obtained in 2016 in this project have been widely disseminated at well-known international conferences:

- The 8th Joint European Magnetics Symposia (JEMS) – JEMS 2016, Glasgow, United Kingdom, 21 – 26 August 2016 – 2 presentations:
    - (PS.1.083) Effect of anisotropy distribution on the hysteresis loops of amorphous glass-coated nanowires – C. Rotărescu, R. Moreno, O. Chubykalo-Fesenko, M. Vázquez, H. Chiriac, N. Lupu, T.-A. Óvári – as a result of the collaboration with the micromagnetics simulation group from Instituto de Ciencia de Materiales de Madrid – ICMM-CSIC, Spain;
    - (PS.1.158) Controlled domain wall dynamics in rapidly solidified amorphous nanowires – M. Țibu, M. Lostun, D.A. Allwood, H. Chiriac, N. Lupu, and T.-A. Óvári – the result of the collaboration with the group of materials physics from the University of Sheffield, UK.
- 16th Czech and Slovak Conference on Magnetism – CSMAG'16, Kosice, Slovakia, 13 – 17 June 2016 – 1 presentation:
    - (P2-42) Formation and motion of domain walls in rapidly solidified amorphous magnetic nanowires – M. Țibu, M. Lostun, D.A. Allwood, H. Chiriac, N. Lupu, and T.-A. Óvári.
- 61st Annual Conference on Magnetism and Magnetic Materials – MMM 2016, New Orleans, Louisiana, United States, 31 October – 4 November 2016 – 1 presentation:
    - (BP-13) Effect of radial anisotropy distribution on the magnetic behavior of rapidly solidified amorphous nanowires – C. Rotărescu, R. Moreno, O. Chubykalo-Fesenko, M. Vázquez, H. Chiriac, N. Lupu, T.-A. Óvári.
- 13th Joint MMM-Intermag Conference, San Diego, California, 11 – 15 January 2016, 1 presentation:
    - (GQ-08) Controlled motion of domain walls in submicron amorphous wires – M. Țibu, M. Lostun, D.A. Allwood, C. Rotărescu, A. Atițoaie, N. Lupu, T.-A. Óvári, H. Chiriac.

The total number of communications related to the dissemination of the project results in 2016 was of 5 presentations at international scientific meetings.

The activities of the project have contributed essentially to the formation of the postdoctoral researchers from the project team. Three postdocs – Dr. Cristian

Rotărescu, Dr. Sorin Corodeanu and Dr. Mihai Țibu – have co-authored the papers published or presented at international conferences.

He have also had excellent results in the international collaborations in the topic of the project, these being financially supported by the EU through a REGPOT type project, in which we have mainly collaborated with the group of Prof. Dan Allwood from the University of Sheffield, UK – one of the world leaders in the investigation of the magnetization processes in nanowires – and with the group of Prof. Manuel Vázquez from Instituto de Ciencia de Materiales de Madrid, ICMM-CSIC, Spain, group which includes one of the leading experts in the field of micromagnetic simulations, Dr. Oksana Chubykalo-Fesenko, who hosted one of our postdoctoral researchers, Dr. Cristian Rotărescu, during two work visits.

Summarizing, all the project objectives have been reached, the obtained results being widely disseminated through publications and conference presentations. The results of our complex studies allow us to move up to the next level, towards a strongly applied research in the field of rapidly solidified amorphous nanowires, in order to investigate their potential use in magnetic domain wall logic devices.

Project Director,

Dr. Tibor-Adrian Óvári